Life Sciences 221 (2019) 284–292

Contents lists available at ScienceDirect

Life Sciences

journal homepage: www.elsevier.com/locate/lifescie

Cytoplasmic ·OH scavenger TA293 attenuates cellular senescence and fibrosis by activating macrophages through oxidized phospholipids/TLR4

Takahiro Sakai*, Jun Imai, Hidetsugu Takagaki, Michio Ui, Shinichi Hatta

Laboratory of Physiological Chemistry, Faculty of Pharmacy, Takasaki University of Health and Welfare, 60 Nakaorui-machi, Takasaki, Gunma 370-0033, Japan

ARTICLE INFO

Keywords:
Cytoplasmic hydroxyl radical
TLR4
Oxidized phospholipid
Macrophage
Inflammation
Oxidative stress

ABSTRACT

Aims: Elucidation of the biological roles of the mitochondrial and cytoplasmic hydroxyl radical (cyto ·OH) is hampered by the absence of site-specific ·OH scavengers. Earlier findings using cyto ·OH scavenger, TA293, indicated that cyto ·OH causes cellular senescence, and senescence-associated secretory phenotype (SASP) factors secreted from cells cause macrophage infiltration, inflammation, and apoptosis. However, we found that macrophage infiltration occurs before senescent cells appear. We therefore aimed to elucidate how cyto ·OH-induces macrophage activation and investigate the mechanism by which activated macrophages cause oxidative stress, inflammation, and apoptosis.

Main methods: In vivo imaging of pyocyanin- and TA293-treated, macrophage-depleted Toll-like receptor 4-knockout ($TLR4^{-/-}$) OKD48- and IDOL-Tg mouse models were used to visualize oxidative stress and inflammation. SA-β-gal and TUNEL staining were used to detect cellular senescence and apoptosis. The mRNA expression of SASP factors were quantified by qRT-PCR. Activation mechanism of cyto ·OH-mediated macrophages was studied by an ex vivo analysis that created macrophage-activated oxidized phospholipids (OxPLs) using $TLR4^{-/-}$ mice.

Key findings: Cyto ·OH produced OxPLs that acted as TLR4 ligands, resulting in macrophage activation. Macrophages were not involved in oxidative stress in tissues or with oxidative damage caused by cyto ·OH, but significantly exacerbated cellular senescence, inflammation, apoptosis, and fibrosis.

Significance: We present a novel mechanism by which cyto ·OH-induced macrophage activation exacerbates cellular senescence, inflammation, apoptosis, and fibrosis independently from the known cyto ·OH-induced cellular senescence pathway. Notably, through suppression of this pathway, TA293 shows promise as a therapeutic agent to prevent fibrosis caused by cyto ·OH-induced oxidative stress.

1. Introduction

Reactive oxygen species (ROS), including superoxides, hydroxyl radicals, peroxides, and singlet oxygen, are generated during aerobic metabolism via the stepwise reduction of molecular oxygen in the mitochondria and the cytoplasm [1]. While ROS are important for signal transduction and homeostasis, overproduction of ROS in response to pathological stimuli can lead to oxidative stress and damage of cellular macromolecules, which promotes inflammation, apoptosis, and tissue destruction. Consequently, ROS are implicated in several pathological conditions associated with chronic inflammation, including cancer, diabetes, neurodegeneration, and fibrosis [1,2].

Hydroxyl radicals (·OH), produced by a metal-catalyzed reaction from hydrogen peroxide, is the most reactive form of ROS and can oxidize every category of macromolecules. In contrast to other ROS, ·OH cannot be removed by an enzymatic reaction, which causes cell and tissue injury [3]. Several studies on the effect of ·OH scavengers such as H_2 [4], dimethylthiourea [5], and natural hydroquinones [6] implicate ·OH in the induction of apoptosis, inflammation, fibrosis, and associated diseases.

Hydroxyl radicals can be produced in different subcellular compartments, as hydrogen peroxide can easily diffuse across the mitochondrial membrane into the cytoplasm, where it reacts with metal ions to generate cytoplasmic ·OH (cyto ·OH). Some studies suggested that mitochondrial ·OH (mito ·OH) and cyto ·OH may play different roles in oxidative stress and trigger distinct pathophysiological effects. Thus, the pathogenesis of neurodegenerative conditions, such as Parkinson's [7] and Alzheimer's [8] diseases, is thought to be associated with the overproduction of cyto rather than mito ·OH. However, research into the specific roles of ·OH radicals generated in different

* Corresponding author.
E-mail address: sakai@takasaki-u.ac.jp (T. Sakai).

https://doi.org/10.1016/j.lfs.2019.02.038
Received 15 November 2018; Received in revised form 5 February 2019; Accepted 17 February 2019
Available online 19 February 2019

subcellular sites has been hampered by the absence of selective scavengers.

Pyocyanin is a redox-active exotoxin of *Pseudomonas aeruginosa* that destroys NADPH and induces oxidative stress and the premature senescence of host cells [19]. Previously, pyocyanin has been shown to generate cyto ·OH [9], which is formed from hydrogen peroxide in the metal-catalyzed Fenton reaction at aqueous interfaces opposite hydrophobic media such as plasma membranes [20]. Using pyocyanin as the inducing agent in an oxidative stress-induced fibrosis model, TA293 and mitoTA293 have been shown to specifically eliminate cyto ·OH and mito ·OH respectively, with TA293 able to suppress macrophage infiltration in tissues with enhanced cyto ·OH-induced oxidative stress [9]. We initially thought that macrophage infiltration in these tissues would be induced by senescence-associated secretory phenotype (SASP) factors secreted from cells that have undergone oxidative damage by ·OH [9]. However, we have found that macrophage infiltration in these tissues is enhanced before the emergence of senescent cells and can be suppressed by TA293. For these reasons, we aimed to investigate the role of macrophages on cyto ·OH-induced oxidative stress, cellular senescence, and inflammation, as well as the effect of cyto ·OH on macrophage activation. We performed in vivo imaging on pyocyanin- and TA293-treated, macrophage-depleted Toll-like receptor 4-knockout ($TLR4^{-/-}$) OKD48- and IDOL-Tg mouse models to visualize oxidative stress and inflammation and SA-β-gal and TUNEL staining to detect cellular senescence and apoptosis.

2. Materials and methods

2.1. Reagents

TA293 was designed by H.T. and synthesized by DIC Corp. (Chiba, Japan); its structure has been published previously [9]. Pyocyanin was purchased from Cayman Chemical (San Diego, CA, USA), and oxidized 1-palmitoyl-2-arachidonoyl-sn-glycero-3-phosphocholine (OxPAPC) was obtained from Hycult Biotech (Uden, The Netherlands).

2.2. Mice

C57BL/6J mice were purchased from CLEA Japan, Inc. (Tokyo, Japan). To monitor oxidative stress and inflammation through luminescence via in vivo imaging, we used Keap1-based oxidative stress detector 48-transgenic (OKD48-Tg) mice and IL-1β-based dual-operating luciferase transgenic (IDOL-Tg) albino C57BL/6J mice, respectively (TransGenic Inc., Kobe, Japan) [10,11]. The role of TLR4 in oxidative stress and inflammation was examined by breeding OKD48-Tg and IDOL-Tg mice with $TLR4^{-/-}$ mice (Oriental Bio Service Inc., Kyoto, Japan) to obtain an F_2 generation. Mice were genotyped using previously described primer sets [10,11]. To generate oxidative stress, mice were treated with pyocyanin delivered as a single intraperitoneal injection (20 mg/kg) or sprayed intratracheally (10 mg/kg) using a microsprayer (Penn-Century, Philadelphia, PA, USA). TA293 was administered intraperitoneally (30 mg/kg) [9]. Only male mice were used in the experiments, although gender was not expected to affect the results. All animal experiments conducted during this study were in strict adherence with the Guide for the Care and Use of Laboratory Animals by US National Institutes of Health (NIH Publications No. 8023, revised 1978). All experimental procedures were approved by the animal experiment ethics committee of our university.

2.3. Isolation of macrophages, non-macrophage cells, and primary embryonic fibroblasts

Mice were sacrificed by cervical dislocation, and the lungs and kidneys were removed, minced with scissors to a fine slurry in 15 mL digestion buffer [RPMI with 10% FBS, 1 mg/mL collagenase (Worthington Biochemical, Freehold, NJ, USA), and 30 g/mL DNase (Sigma, St. Louis, Missouri USA)], and incubated for 30 min at 37 °C. The cell suspension was centrifuged, and the pellet was resuspended in 40% Percoll (GE Healthcare Life Sciences, Piscataway, NJ, USA), overlaid with 70% Percoll, and centrifuged again to separate the macrophage-enriched fraction from the cell fraction containing epithelial and endothelial cells.

To induce peritoneal macrophages, mice were administered 2 mL of 4% thioglycollate (Nissui, Tokyo, Japan) intraperitoneally and sacrificed after 4 days. Macrophages were collected by irrigation of the peritoneal cavity with 5 mL phosphate buffered saline (PBS) and purified using the Percoll gradient as described above.

Primary mouse embryonic fibroblasts (MEFs) were obtained from E13.5 embryos of C57BL/6J mice and treated with pyocyanin with or without TA293.

2.4. Measurement of senescence-associated β-galactosidase (SA-β-gal) activity

Senescent cells in the lungs and kidneys were assessed by SA-β-gal staining using the Senescence Detection Kit (BioVision, Mountain View, CA, USA) following the manufacturer's instructions. Briefly, frozen tissue sections were fixed in 2% formaldehyde and incubated with staining solution for 16 h at 37 °C. Subsequently the slides were washed with PBS and mounted with Permount (Fisher Scientific, New Jersey, USA). The cells that were stained as positive were counted under a microscope at 20× magnification in five fields for each experimental condition.

2.5. Western blotting

Tissues and cells were homogenized on ice in RIPA buffer (20 mM Tris-HCl [pH 7.4], 150 mM NaCl, 1% NP-40, 1% sodium deoxycholate, and 0.1% SDS) containing protease and phosphatase inhibitors (cOmplete Mini and phosSTOP, respectively; Roche Diagnostics GmbH, Mannheim, Germany), and centrifuged at 11,000 × *g* for 30 min. Protein concentration in supernatants were estimated using the Bradford assay (Bio-Rad, Hercules, CA, USA). Western blotting was conducted following standard procedures, using primary antibodies against p16INK4a (Bioworld Technology, St. Louis Park, MN, USA), p21Waf1/Cip1 (Santa Cruz Biotechnology, Dallas, TX, USA), CD68 (Serotec, Raleigh, NC, USA), cleaved caspase-3, phospho-IκB, α-SMA, collagen alpha-1(I), and β-actin (Cell Signaling Technology, Beverly, MA, USA), diluted 1:1000. After incubation with HRP-linked secondary antibodies (Cell Signaling Technology), signals were detected using ECL Plus Western Blotting Detection Reagents (GE Healthcare Life Sciences).

2.6. Preparation and detection of oxidized pulmonary surfactant phospholipids (SPLs)

Oxidized SPLs were prepared by adding Surfacten (Mitsubishi Tanabe Pharma Corp., Osaka, Japan) after inducing the Fenton reaction using 0.2 mM $FeSO_4$ and 1 mM H_2O_2 in the presence of TA293 or vehicle for 4 min at 20 °C. Oxidized SPLs were detected by the EO6 binding assay as described previously [12]. Briefly, Oxidized SPLs were incubated with the EO6 antibody (Avanti Polar Lipids, Alabaster, AL, USA) for 2 h at room temperature, and binding was detected using a goat-anti-mouse AP-labeled IgM (Sigma) for 1 h at room temperature, followed by 33% LumiPhos Plus (Lumigen Inc., Southfield, MI, USA) for 90 min. Light emission was measured using a WALLAC VIKTOR II luminometer (PerkinElmer, Waltham, MA, USA) and expressed as relative light units (RLU)/100 ms.

2.7. Macrophage depletion

Clodronate liposomes (FormuMax Scientific, Palo Alto, CA, USA)

were administered to mice (50 μL/g intraperitoneally) after fasting. Macrophage depletion was confirmed 24 h later by western blotting using the anti-CD68 antibody.

2.8. In vivo imaging analysis

OKD48-Tg and IDOL-Tg mice were injected intraperitoneally with D-luciferin in PBS (150 mg/kg body weight), 24 h after pyocyanin administration with or without TA293. Whole-body imaging was then performed utilizing the IVIS Lumina II in vivo imaging system (Caliper Life Sciences, Hopkinton, MA, USA). Mice were sacrificed 10 min after luciferin injection, and kidneys and lungs were collected, immersed in 0.3 mg/mL D-luciferin, and analyzed.

2.9. Histology, immunohistochemistry, and detection of fibrosis and apoptosis

Histological analysis was performed on tissues fixed in 4% buffered formalin, cut into 3–5 μm thick sections, and stained with hematoxylin and eosin (H&E). Fibrotic zones were detected by Masson's trichrome staining under a NIS-Elements microscope (Nikon Instruments, Tokyo, Japan). Immunohistochemistry was performed in 5-μm-thick sections of paraffin-embedded samples, during which macrophages were identified using anti-F4/80 antibodies (Abcam, Cambridge, MA, UK), and OxPLs were detected using the EO6 antibody. Apoptosis was assessed via TUNEL assay using the ApopTag Peroxidase In Situ Apoptosis Detection Kit (Millipore, Billerica, MA, USA), and apoptotic cells were counted under a NIS-Elements microscope.

2.10. Evaluation of oxidative stress

Malondialdehyde (MDA) generation was determined by the TBARS method [13] using an MDA assay kit (JaICA, Fukuroi, Japan). The levels of 8-OHdG in serum and tissue homogenates were measured by ELISA (8-OHdG Check; JaICA) and normalized to that of creatinine. Serum and tissue protein carbonyl contents were assessed by ELISA (Immundiagnostik AG, Bensheim, Germany) following the manufacturer's instructions and calculated based on a standard curve constructed using oxidized bovine serum albumin (BSA).

2.11. RNA isolation and quantitative reverse transcription (qRT-PCR)

Total RNA was isolated from lung and kidney tissue, macrophages and crude non-macrophage cells from lung and kidney, or peritoneal macrophages (2.5×10^5 cells per well of a 6-well plate) stimulated in vitro with pyocyanin (10 μM), OxPAPC (10 μg/mL), and/or TA293 (100 μM) for 6 h, and MEF stimulated in vitro with pyocyanin (10 μM), and/or TA293 (100 μM) for 72 h, using Isogen reagent (Takara Bio, Kyoto, Japan) according to the manufacturer's protocol. RNA (1 μg) was reverse-transcribed using the RNA LA PCR Kit (Takara Bio), and mRNA expression was analyzed by qRT-PCR using the Thunderbird SYBR qPCR Mix (Toyobo, Osaka, Japan) and previously described primers [9]. Five samples were used in each experiment.

2.12. Ex vivo ESR measurements

The lungs were separated from sacrificed mice, placed in a plastic vessel, and kept on ice. Following homogenization, the organs were pre-incubated in 0.3 mL PBS containing 0.1 M 5,5-dimethyl-1-pyrroline N-oxide (DMPO) for 7 min at 20 °C. Subsequently, the mixture was transferred to a glass capillary for ESR experiments. These samples were measured using an ESR JES-REIX X-band spectrometer (JEOL, Tokyo, Japan). The O_2^- detection conditions were: field, 336 ± 5 mT width; power, 4 mW; field modulation, 0.079 mT; time constant, 0.1 s; and amplitude, 250. The ·OH detection conditions were: field, 336 ± 5 mT width; power, 4 mW; field modulation, 0.200 mT; time constant, 0.1 s; and amplitude, 500. A manganese signal was used for the external standard.

2.13. Measurement of H_2O_2 in tissue

Quantitation of H_2O_2 was evaluated using OxiSelect™ Hydrogen Peroxide/Peroxidase Assay Kit (Cell Biolabs, Inc. San Diego, CA, USA). Tissue homogenates were prepared by homogenizing the lung samples in assay buffer and recovering the supernatants by centrifugation. Fifty μl of tissue homogenate and 50 μL of hydrogen peroxide working solution content were added and incubated for 30 min at room temperature protected from light. Absorbance was then measured at 540 nm to quantify H_2O_2 in tissue homogenate.

2.14. Statistical analysis

The data are presented as the mean ± standard error of the mean (SEM) based on five independent experiments. Statistical analysis was performed by one-way analysis of variance (ANOVA) using Excel (BellCurve, Tokyo, Japan) and IBM SPSS (Tokyo, Japan) software. $P < 0.05$ was considered statistically significant.

3. Results

3.1. Inflammation induced by cyto ·OH is mediated by macrophages

The TA293 and mitoTA293 developed by our group did not eliminate O_2^- or H_2O_2 in vivo in wild-type (WT) mice (Fig. S1A, B), but instead specifically eliminated cyto ·OH and mito ·OH, respectively (Fig. S1C). It has been demonstrated that TA293 attenuated oxidative stress and suppressed macrophage infiltration induced by cyto ·OH in the lungs and kidneys of mice treated with pyocyanin, whereas mitoTA293 was not capable of suppressing oxidative stress or macrophage infiltration [9]. We therefore used the OKD48-Tg mice to determine the effect of pyocyanin and TA293 on oxidative stress (Fig. S2A, B), and WT mice to determine the cellular senescence and macrophage infiltration in the lungs and kidneys (Fig. S2C, D). Our findings were similar at 24 h after administration of pyocyanin and/or TA293. Additionally, we observed that oxidative stress and macrophage infiltration increased in lungs and kidneys 3 h after pyocyanin administration and further increased over time (Fig. S3A, B), whereas SA-β-gal-positive cells increased 12 h after pyocyanin administration and further increased over time (Fig. S3C). These results indicate that cyto ·OH-dependent macrophage infiltration in tissues with oxidative damage is not solely attributed to SASP factors secreted from senescent cells and suggest that cyto ·OH may be involved in macrophage activation. Based on the results shown in Fig. S2B, we next aimed to determine whether macrophages mediated oxidative stress due to cyto ·OH and examined the effects of pyocyanin in the lungs and kidneys from macrophage-depleted and control OKD48-Tg mice. Pyocyanin induced oxidative stress in both groups, which was inhibited by TA293 (Fig. 1A, B), suggesting that macrophages were not involved in oxidative stress caused by cyto ·OH. However, HE and SA-β-gal staining of lung samples showed that, upon pyocyanin administration, the increase in the alveolar wall thickness and the damage to the alveolar structures, as well as the number of SA-β-gal-positive blue cells, were lower in macrophage-depleted lungs than in control lungs, indicating that macrophages did contribute to cyto ·OH-induced tissue damage and cellular senescence. In the kidneys, the absence of macrophages prevented the pyocyanin-induced atrophy of renal tubules and edema of the renal tubules, and also prevented the increase in the number of SA-β-gal-positive blue cells. These effects were, however, more pronounced in the presence of TA293 (Fig. 1C, D). Further, macrophage depletion resulted in a decrease in the pyocyanin-induced expression of the cell cycle inhibitors p16INK4a (p16) and p21Waf1/Cip1 (p21), as well as the phosphorylation of IκB (Fig. 1E) in the lungs and kidneys of

pyocyanin-treated mice, suggesting that macrophages exacerbated the organ injury and cellular senescence caused by cyto ·OH.

Pyocyanin increased the expression of p16 and p21 specifically in non-macrophage cells, while upregulating IκB phosphorylation in both macrophage and non-macrophage cell fractions of the lungs and kidneys (Fig. S4A). Notably, TA293 suppressed these effects (Fig. S4A). Furthermore, pyocyanin upregulated the mRNA expression of SASP factors in both macrophage and non-macrophage cells, and treatment with TA293 inhibited this upregulation (Fig. S4B). These findings suggest that cyto ·OH triggers senescence in non-macrophage cells, which secrete SASP factors such as CCL2 to attract and activate macrophages. In turn, activated macrophages release pro-inflammatory mediators such as IL-1β, IL-6, and TNFα, thus sustaining inflammation in the lungs and kidneys.

In addition, in the lungs and kidneys of the IDOL-Tg mice, inflammation was suppressed by macrophage depletion as well as treatment with TA293 (Fig. 1F) but not mitoTA293 (Fig. S5A), providing further evidence that cyto ·OH-induced inflammation is mediated by macrophages. Moreover, macrophage infiltration was found to be involved in the activation of apoptosis by cyto ·OH and was associated with a decrease in pyocyanin-induced TUNEL staining (Fig. 1G) and caspase 3 cleavage (Fig. 1H) in macrophage-depleted mice. At the same time, TA293 completely suppressed pyocyanin-induced apoptosis (Fig. 1F, G), whereas mitoTA293 did not (Fig. S5B). These results indicate that macrophages are involved in the exacerbation of apoptosis in the lungs and kidneys damaged by cyto ·OH.

Overall, these findings reveal the role of macrophages in mediating the effects of cyto ·OH. While macrophages are not directly involved in causing oxidative stress in tissues in response to cyto ·OH, they are likely to be activated by SASP factor secreted by senescent cells along with other pathways, further aggravating the inflammation process. Inflammatory cytokines produced by activated macrophages aggravate cellular senescence and inflammation, resulting in apoptosis and further damage of pulmonary and renal tissues.

3.2. TLR4 is involved in macrophage activation by cyto ·OH

In order to find factors besides SASP factor that activate macrophages in tissues in which oxidative stress is induced due to cyto ·OH, we examined the oxidation profile of cyto ·OH in mice at the molecular level 6 h after administering pyocyanin with or without TA293. Although pyocyanin caused DNA and protein oxidation in serum, lungs, and kidneys, TA293 did not suppress it (Fig. S6A, B), suggesting that cyto ·OH does not directly oxidize DNA and proteins. However, TA293 reversed the pyocyanin-induced increase in MDA, a major oxidation product of low-density lipoprotein (LDL) (Fig. S6C), and the reactivity of the EO6 antibody specific for oxidized phospholipids (OxPLs) (Fig. 2A, B) in lung and kidney 6 h after administering pyocyanin with

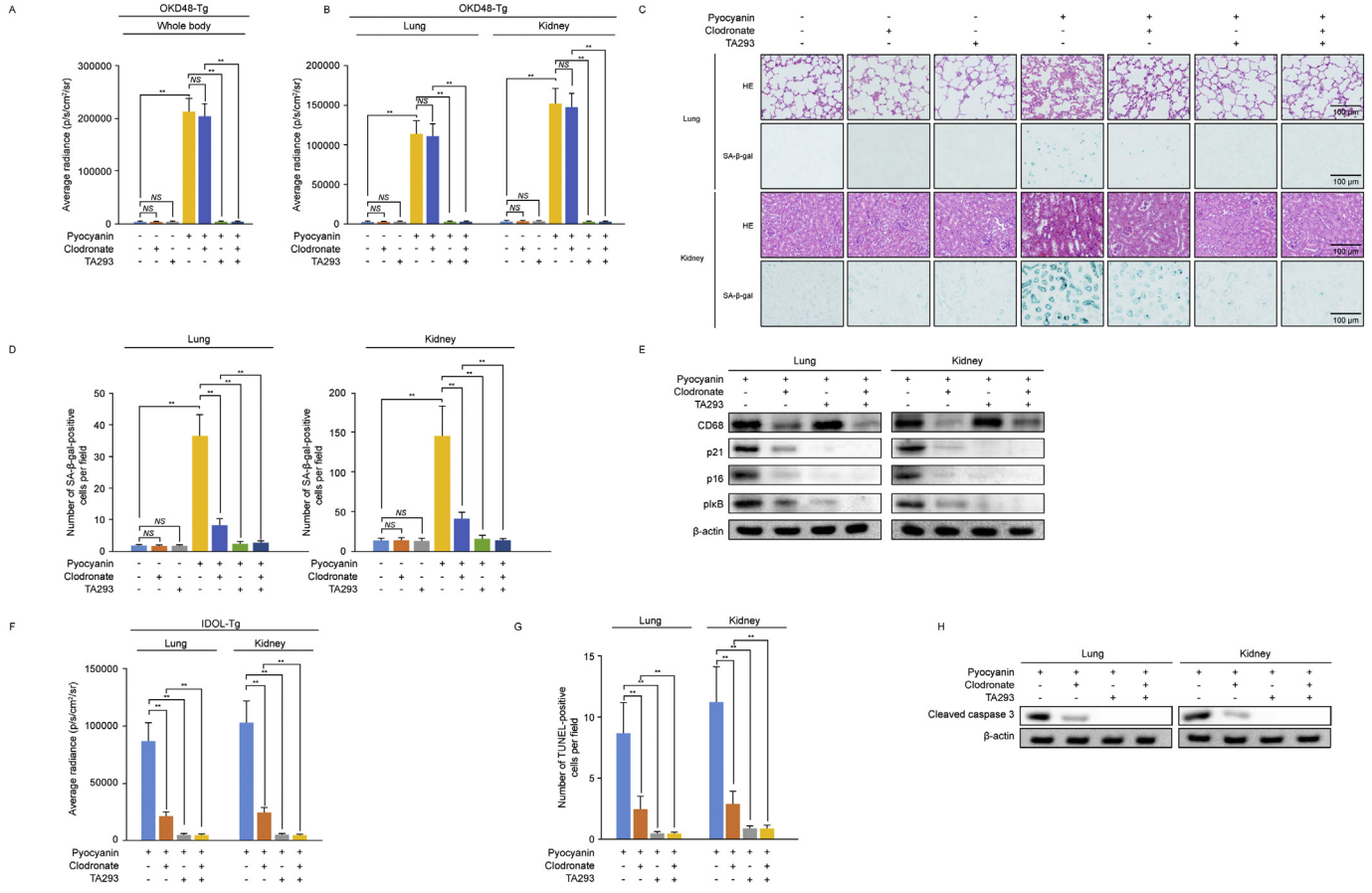

Fig. 1. Cellular senescence, inflammation, and apoptosis, but not oxidative stress, caused by cyto ·OH is mediated by macrophages. Mice were treated with clodronate liposomes for 24 h, followed by the administration of pyocyanin and/or TA293. The animals were sacrificed 24 h after administration of pyocyanin and/or TA293 and oxidative stress was quantified based on luminescence activity in (A) whole body, as well as (B) the lungs and kidneys of OKD48-Tg mice. (C) Lung and kidney tissue sections of C57BL/6J mice were analyzed for histopathology (H&E staining) and cellular senescence (SA-β-gal staining). (D) Number of senescent SA-β-gal-positive blue cells in the lungs and kidneys. (E) Expression of the macrophage marker CD68, senescence markers p16 and p21, and phospho-IκB, an indicator of NF-κB signaling activation, determined by western blotting in C57BL/6J mice. (F) Determination of inflammation in the whole body of macrophage-depleted IDOL-Tg mice. (G, H) Apoptosis evaluated by TUNEL staining (G) and cleaved caspase-3 levels (H) in the lungs and kidneys of clodronate-treated or untreated C57BL/6J mice 72 h after pyocyanin and/or TA293 injection. The data are presented as the mean ± SEM ($n = 5$ per group); $^{**}p < 0.01$; NS, not significant. (For interpretation of the references to color in this figure legend, the reader is referred to the web version of this article.)

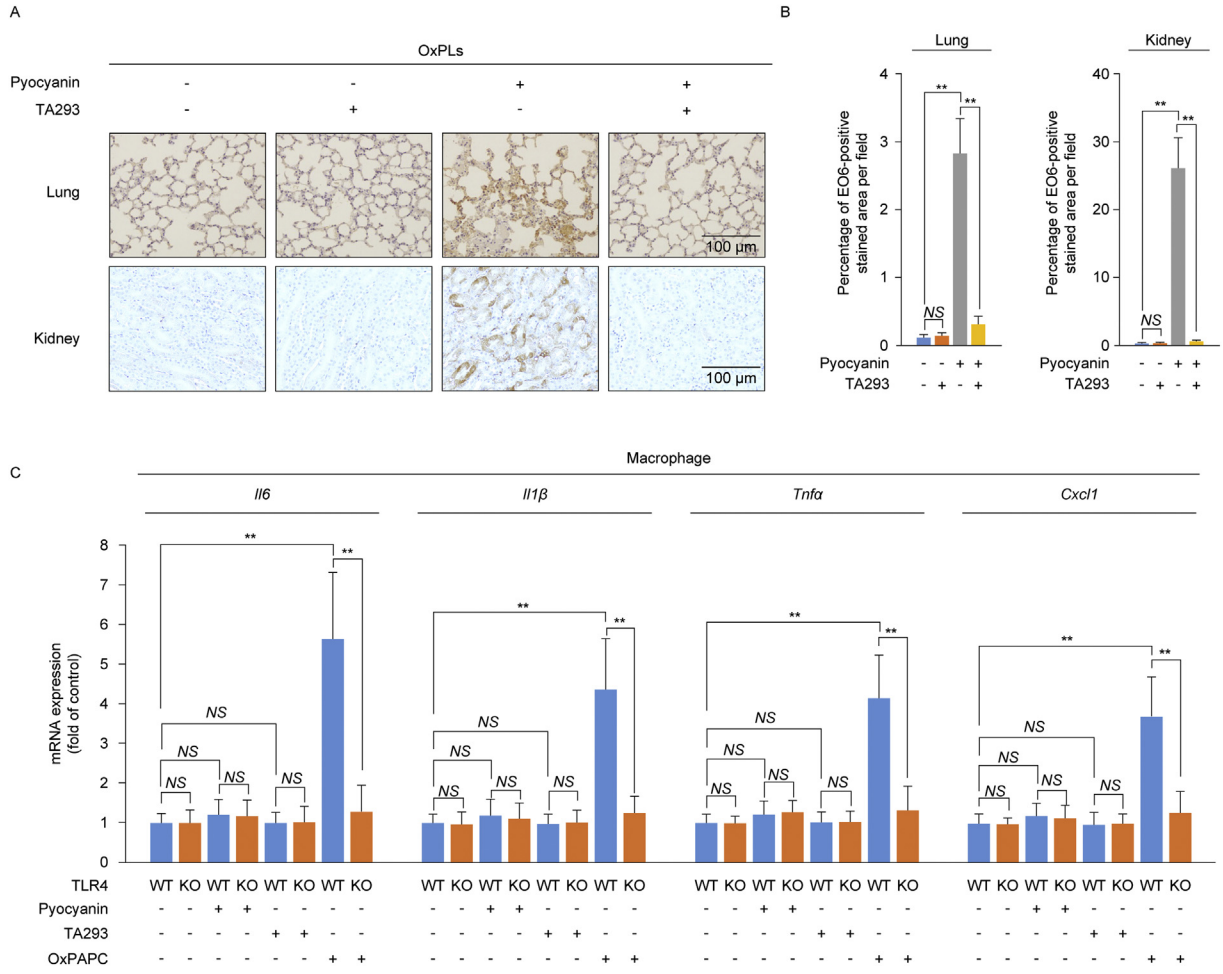

Fig. 2. Oxidized phospholipids (OxPLs) produced by cyto ·OH are involved in macrophage activation. (A, B) OxPLs production detected by immunohistochemistry with the EO6 antibody in the lungs and kidneys of C57BL/6J mice 6 h after pyocyanin and/or TA293 administration. (C) Expression of *Il6*, *Il1b*, *Tnfa*, and *Cxcl1* mRNA in peritoneal macrophages isolated from WT or TLR4$^{-/-}$ mice 6 h after in vitro exposure to pyocyanin or OxPAPC and/or TA293. The data are presented as the mean ± SEM (n = 5 per group); $^{**}p < 0.01$; NS, not significant.

or without TA293, indicating that cyto ·OH causes lipid peroxidation.

It is known that oxidized LDL and OxPLs can activate macrophages through TLR4 signaling [12]. To examine whether this was the case in our model, peritoneal macrophages from WT and TLR4$^{-/-}$ mice were treated 6 h ex vivo with a mixture of biologically active oxidized phospholipids (pyocyanin, TA293, and OxPAPC), and the mRNA expression of inflammatory cytokines was analyzed (Fig. 2C). Pyocyanin and TA293 did not affect cytokine expression in either WT or TLR4$^{-/-}$ macrophages, whereas OxPAPC significantly upregulated mRNA levels of all examined inflammatory cytokines in WT macrophages, but much less in TLR4$^{-/-}$ macrophages (Fig. 2C).

Together, these results suggest that in vivo, cyto ·OH induces lipid peroxidation and generation of OxPLs, which then activate macrophages via TLR4 to upregulate the production of inflammatory cytokines.

3.3. TLR4 mediates oxidative stress, cellular senescence, inflammation, and apoptosis induced by cyto ·OH

In both WT and TLR4$^{-/-}$ OKD48-Tg mice, pyocyanin induced oxidative stress via cyto ·OH (Fig. 3A, B), which TA293 reversed. TA293 also reversed the pyocyanin-induced damage to the alveolar walls in the lungs and the atrophy of the renal tubules in the kidneys, as well as the increased number of SA-β-gal-positive blue cells in the lungs and kidneys (Fig. 3C, D). However, pyocyanin-induced macrophage infiltration decreased (Fig. 3E) and phosphorylation of IκB was determined to be absent in the macrophage fraction (Fig. 3F) of the lungs and kidneys from TLR4$^{-/-}$ mice when compared to that in wild-type (WT) mice. Notably, this correlated with decreased inflammation observed in TLR4$^{-/-}$ IDOL-Tg mice (Fig. S7). The expression of p16 and p21, and phosphorylation of IκB were increased by pyocyanin and suppressed by TA293 both in WT and TLR4$^{-/-}$ non-macrophage cells (Fig. 3F). Pyocyanin-induced apoptosis was lower in TLR4$^{-/-}$ mice (Fig. 3G, H), and the number of apoptotic cells was further reduced by TA293 (Fig. 3G, H). In contrast, no TLR4-dependent changes were observed in the OxPLs levels as determined by the reactivity to anti-E06 antibody visualized as brown staining, as there was a similar increase with pyocyanin and decrease with TA293 in both WT and TLR4$^{-/-}$ mice (Fig. 3I, J). Together, these data suggest that TLR4 is not directly involved in cyto ·OH-induced oxidative stress, cellular senescence, and OxPLs production, but mediates the infiltration/activation of macrophages, inflammation, and apoptosis in mouse lungs and kidneys.

To confirm these results, we tested whether using OxPLs as TLR4 ligands could reproduce these effects in vivo. OxPLs were prepared from pulmonary SPLs by triggering the Fenton reaction in cell-free conditions to generate ·OH, which was suppressed by TA293 (Fig. 4A). Spraying oxidized SPLs into mouse lungs exhibited no effect on oxidative stress, the number of SA-β-gal-positive cells or the expression of p16 and p21 (Fig. S8A, Fig. 4B, C, E). However, Oxidized SPLs, but not oxidized SPLs incubated with TA293, increased the infiltration of F4/

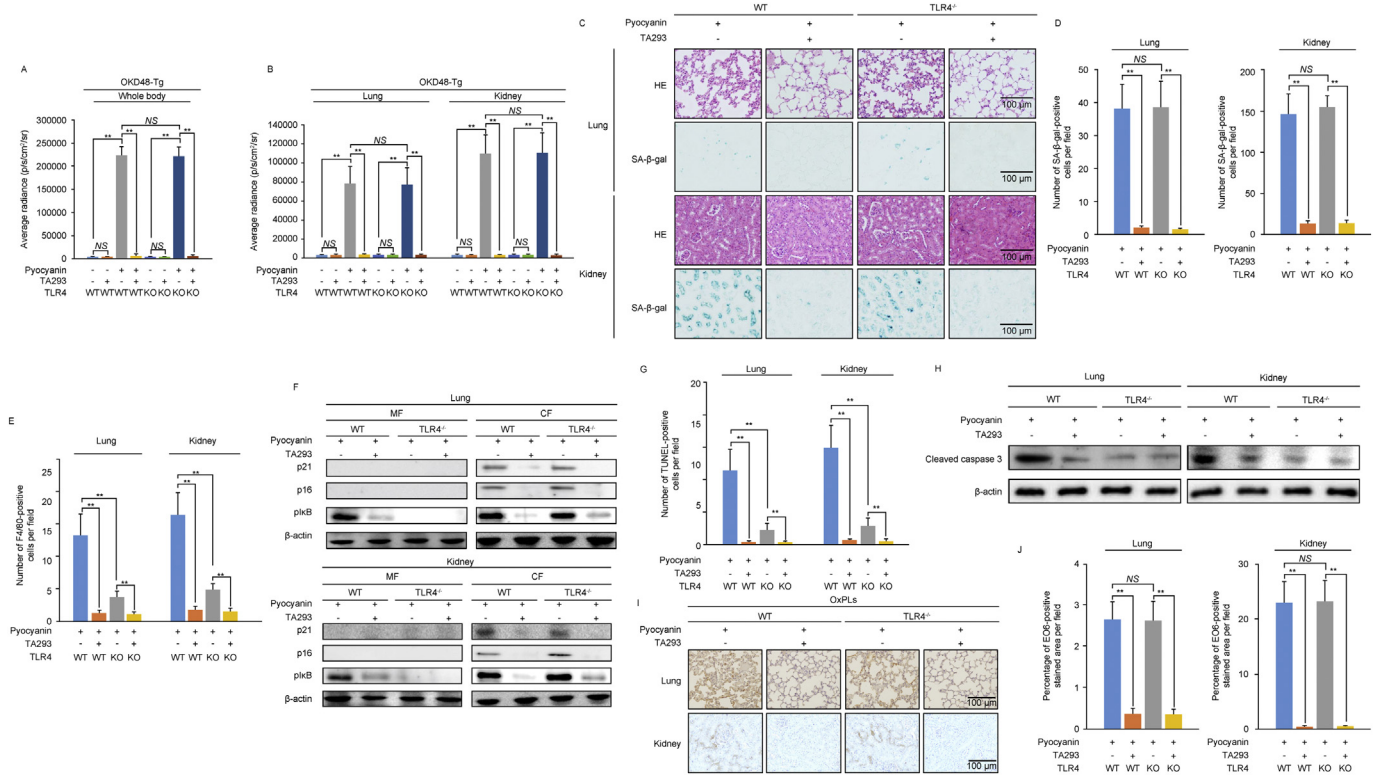

Fig. 3. TLR4 mediates macrophage activation, inflammation, and apoptosis, but not oxidative stress, cellular senescence, or OxPL production induced by cyto ·OH. Mice were treated with pyocyanin with or without TA293 for 24 h (A–F), 72 h (G, H) or 6 h (I, J). (a, b) Determination of luminescence in (A) the whole body and (B) lungs and kidneys of WT and TLR4$^{-/-}$ OKD48-Tg mice. (C) Histopathology (H&E staining) and cellular senescence (SA-β-gal staining) in WT and TLR4$^{-/-}$ mice. (D) Number of senescent SA-β-gal-positive blue cells in the lungs and kidneys. (E) Quantitation of macrophage infiltration in WT and TLR4$^{-/-}$ mice analyzed by immunohistochemistry using the F4/80 antibody. (F) Expression of p16, p21, and phospho-IκB in the macrophage fraction (MF) and crude non-macrophage cell fraction (CF) from WT and TLR4$^{-/-}$ mice. (G, H) Apoptosis in the lungs and kidneys of WT and TLR4$^{-/-}$ mice evaluated by TUNEL staining (G) and cleaved caspase-3 expression levels (H). (I, J) EO6 staining in WT and TLR4$^{-/-}$ mice. (I) Detection and (J) quantification of OxPLs in the lungs and kidney. The data are presented as the mean ± SEM (n = 5 per group); $^{**}p < 0.01$; NS, not significant. (For interpretation of the references to color in this figure legend, the reader is referred to the web version of this article.)

80-positive cells and IκB phosphorylation (Figs. 4D, E, and S8B). These findings indicate that oxidized SPLs are produced by ·OH induce infiltration and activation of macrophages in the lung (Fig. 4D, E), which is consistent with the involvement of TLR4 signaling (Fig. 3) and was further confirmed in the experiments with TLR4$^{-/-}$ mice (Figs. 4F–I and S9A, B).

Overall, these data suggest that OxPLs generated by cyto ·OH are not involved in oxidative stress but may act as TLR4 ligands to activate macrophages and promote inflammation, which aggravates cellular senescence and apoptosis.

3.4. Cyto ·OH induces renal and pulmonary fibrosis via TLR4 signaling in macrophages

It is known that ROS is closely associated with the onset and progression of fibrosis, in part through upregulation of cytokines of the transforming growth factor-β (TGF-β) family, which induce the expression of extracellular matrix (ECM) proteins [14]. To examine the effect of cyto ·OH on tissue fibrosis, we treated WT and TLR4$^{-/-}$ mice for 21 days with pyocyanin, with or without TA293 or clodronate pretreatment, and compared the size of the fibrotic areas and expression of fibrogenic factors in the lungs and kidneys. The results indicate that pyocyanin induced fibrosis in WT mice, as determined by the increase in blue staining in the lungs and kidneys, but not in macrophage-depleted or TLR4$^{-/-}$ mice, and the effect was abrogated by TA293 (Fig. 5A, B).

Consistently with the increase in fibrosis, pyocyanin was found to upregulate the α-smooth muscle actin (α-SMA) and soluble collagen alpha-1(I) chain expressed by activated fibroblasts at the fibrosis site in WT, but not in TLR4$^{-/-}$ or macrophage-depleted mice, and this upregulation could be inhibited by TA293 (Fig. 5C). Furthermore, on day 7, pyocyanin induced mRNA expression of *Tgfb1* (Fig. 5D) and plasminogen activator inhibitor-1 (*PAI-1*, also known as *Serpine1*) (Fig. 5E), two genes known to promote fibrosis progression, in WT but not in TLR4$^{-/-}$ or macrophage-depleted mice. However, TA293 reversed pyocyanin-induced upregulation of pro-fibrotic factors (Fig. 5D, E). As fibroblasts are the main players in fibrosis and they secrete TGF-β and PAI-1, which act on fibroblasts through an autocrine loop, we analyzed the *Tgfb1* and *Serpine1* expression in MEFs treated with pyocyanin, with or without TA293. The results indicated that pyocyanin increased the transcription of *Tgfb1* and *Serpine1*, which was inhibited by TA293, but not by mitoTA293 (Fig. 5F, G).

Cumulatively, these data indicate that cyto ·OH triggers fibrosis through activation of the TLR4 pathway in macrophages, which can be attenuated by TA293.

4. Discussion

The interplay between ROS, oxidative stress, inflammation, and fibrosis is implicated in the pathogenesis of various disorders [15], including chronic kidney disease and acute respiratory distress syndrome [16,17]. The few reports on the fibrogenic effects of the ·OH radical provided only indirect evidence suggesting that ·OH scavengers like hydrogen-rich saline and suplatast tosilate can be protective in the case of lipopolysaccharide-induced fibrosis or in the hyperoxic lung injury/pulmonary fibrosis model [4,18]. However, the fundamental

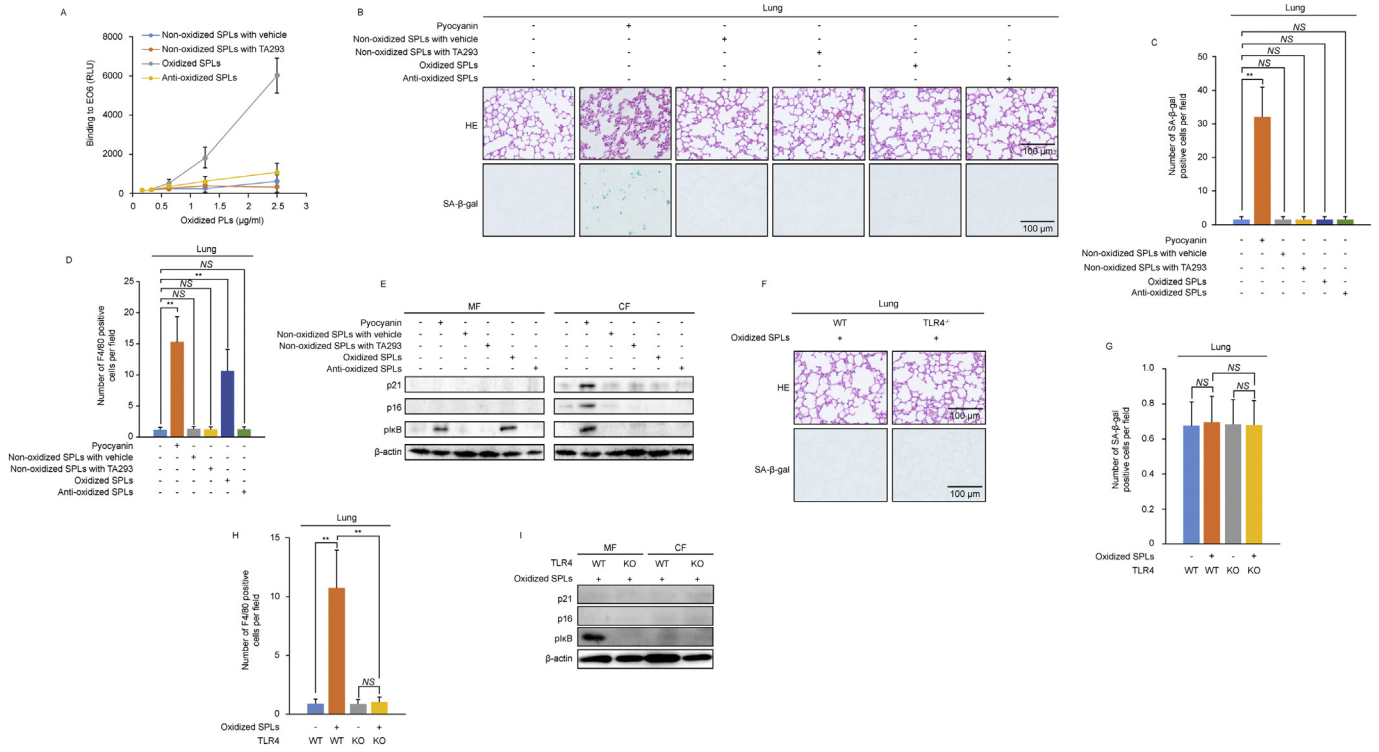

Fig. 4. Oxidized SPLs trigger cytokine production and macrophage infiltration via TLR4, but do not lead to cellular senescence. (A) Binding of the EO6 antibody to confirm the presence of EO6-positive OxPLs in the oxidized SPLs in cell free system. EO6 binding is expressed in relative light units (RLU). Non-oxidized SPLs with vehicle and non-oxidized SPLs with TA293 produced in the absence of a Fenton reaction, and oxidized SPLs, or anti- oxidized SPLs in the presence of TA293 produced by Fenton reaction. (B–I) Various SPLs as confirmed in panel A were delivered intratracheally (50 mg/kg) into WT or TLR4$^{-/-}$ (KO) mice using a microsprayer, and lungs were analyzed after 24 h. Histopathology (H&E staining) and cellular senescence (SA-β-gal staining in WT mice (C, D). Number of senescent SA-β-gal-positive blue cells in the lungs and kidneys (C) and F4/80-positive macrophages in the lungs of WT mice (D). Expression of p16, p21, and phospho-IκB in the macrophage fraction (MF) and crude non-macrophage cell fraction (CF) from the lungs of WT mice was determined by western blotting (E). H&E staining and SA-β-gal staining in the lungs of WT and TLR4$^{-/-}$ mice treated with oxidized SPLs (F). Number of senescent SA-β-gal-positive blue cells in the lungs and kidneys (G) and F4/80-positive macrophages (H) in the lungs of WT and TLR4$^{-/-}$ mice treated with oxidized SPLs. Western blotting analysis of p16, p21, and phospho-IκB expression in the MF and CF of the lungs from WT and TLR4$^{-/-}$ mice treated with oxidized SPLs (I). The data are presented as the mean ± SEM ($n = 5$ per group); $^{**}p < 0.01$; NS, not significant. (For interpretation of the references to color in this figure legend, the reader is referred to the web version of this article.)

mechanism involved was not elucidated, nor were the differences between the ·OH generated in various subcellular compartments analyzed.

In this study, we showed that cyto ·OH induced cellular senescence, inflammation, apoptosis and fibrosis in mouse lungs and kidneys, which were prevented by TA293, a scavenger that specifically targets ·OH radicals produced by pyocyanin in the cytoplasm. By addressing the molecular mechanisms underlying the pro-inflammatory and pro-fibrotic effects of cyto ·OH, we revealed preferential oxidation of lipids generating OxPLs, which caused SASP cytokines to be released by non-macrophage cells of the lungs and kidneys to activate TLR4 signaling in macrophages. This cascade of events resulted in the transcriptional upregulation of pro-fibrotic TGF-β and PAI-1, and the enhanced expression of α-SMA and soluble collagen alpha 1(I) chain, leading to renal and pulmonary fibrosis. Our results are consistent with previous findings that OxPLs can directly trigger cytokine production in macrophages via TLR4, thus modulating the severity of acute lung injury in mice [12].

Although we found that TLR4 was not directly involved in oxidative stress, cellular senescence, or OxPL production induced by cyto ·OH, it played a role in the activation of macrophages, apoptosis, inflammation and fibrosis. These conclusions are supported by a previous report that TLR4 signaling is involved in angiotensin II-induced renal injury and fibrosis through ROS production and macrophage-mediated inflammation [21] and are in line with the function of TLR4 as a sensor and signal transducer during oxidative stress [22].

Based on our results, we propose a model integrating cyto ·OH-induced oxidative stress, cellular senescence, inflammation, apoptosis, and fibrogenesis (Fig. 6). Cyto ·OH causes oxidative damage in non-macrophage cells, promoting their senescence and release of SASP factors to attract macrophages, while OxPLs generated by lipid peroxidation trigger TLR4 signaling in activated macrophages infiltrating the lungs and kidneys. Inflammatory cytokines secreted by stimulated macrophages promote infiltration and exacerbate inflammation and cellular senescence, leading to apoptosis, remodeling of tissues damaged by oxidative stress, and ultimately, fibrosis.

In this study, ROS were generated by pyocyanin, but we believe that a similar pathway can be triggered by the activity of NADPH oxidases (NOX), which may participate in the production of cyto ·OH through oxidation of intracellular NADPH, generation of O_2^- and then H_2O_2 to be utilized in the Fenton reaction [23]. Among the ROS-producing enzymes, NOX appear to play a key role during fibrosis [24]. Consistent with this, NOX expression is upregulated in mouse lungs subjected to non-infectious injury and in human idiopathic pulmonary fibrosis [25]. It has also been shown that oxidative stress increases NOX synthesis, which corresponds to the upregulation of TGF-β expression and fibronectin deposition in mouse proximal tubular cells, induction of renal fibrosis, and deterioration of kidney function [26].

TGF-β is considered a “master switch” of fibrogenesis in many tissues, including the heart, kidney, and lung [14]. ROS are shown to be involved in TGF-β-mediated fibrosis, either through direct activation of TGF-β or indirectly via enhanced inflammation [15]. Our results indicate that cyto ·OH upregulates TGF-β expression in mouse renal and pulmonary tissues, as well as in fibroblasts, the principal cell type

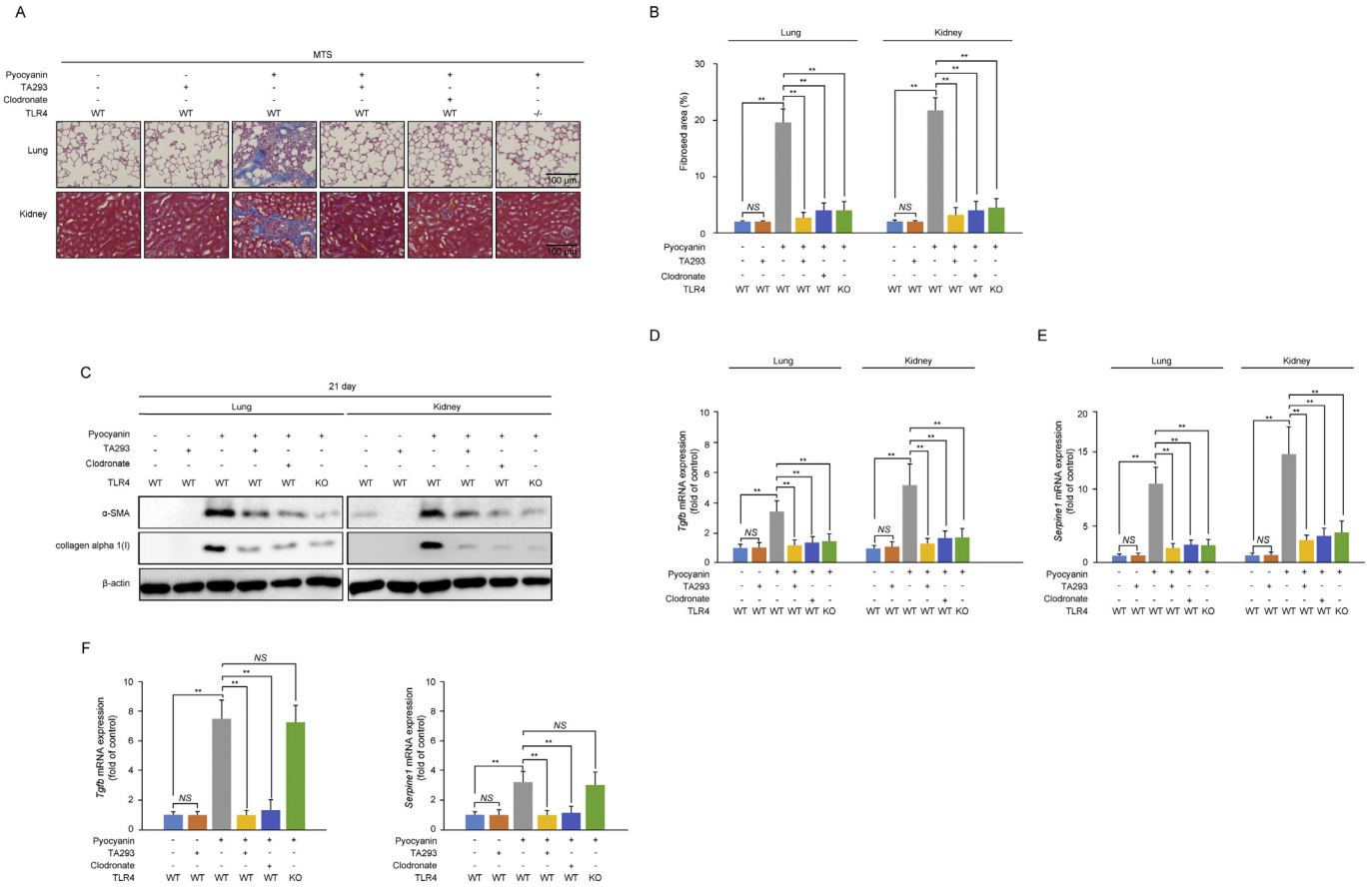

Fig. 5. Cyto ·OH induces pulmonary and renal fibrosis via OxPL/TLR4 signaling in macrophages. (A–E) WT and TLR4$^{-/-}$ mice were treated with clodronate for 24 h, followed by administration of pyocyanin with or without TA293 and analysis of renal and pulmonary fibrosis 21 days later. (A, B) Images (A) and semi-quantitative analysis (B) of fibrotic areas in kidney and lung tissues after Masson's trichrome staining. (C) Expression of α-SMA and collagen alpha 1 (I) analyzed by western blotting. (D, E) *Tgfb1* (D) and *Serpine1* (E) mRNA expression day 7 after administration of pyocyanin with or without TA293 analyzed by qRT-PCR. (F, G) MEFs were stimulated by pyocyanin (10 μM) with or without 100 μM TA293 or mitoTA293 for 72 h and the mRNA expression of *Tgfb1* (F) and *Serpine1* (G) was analyzed by qRT-PCR. The data are presented as the mean ± SEM (n = 5 per group); $^{**}p < 0.01$; NS, not significant.

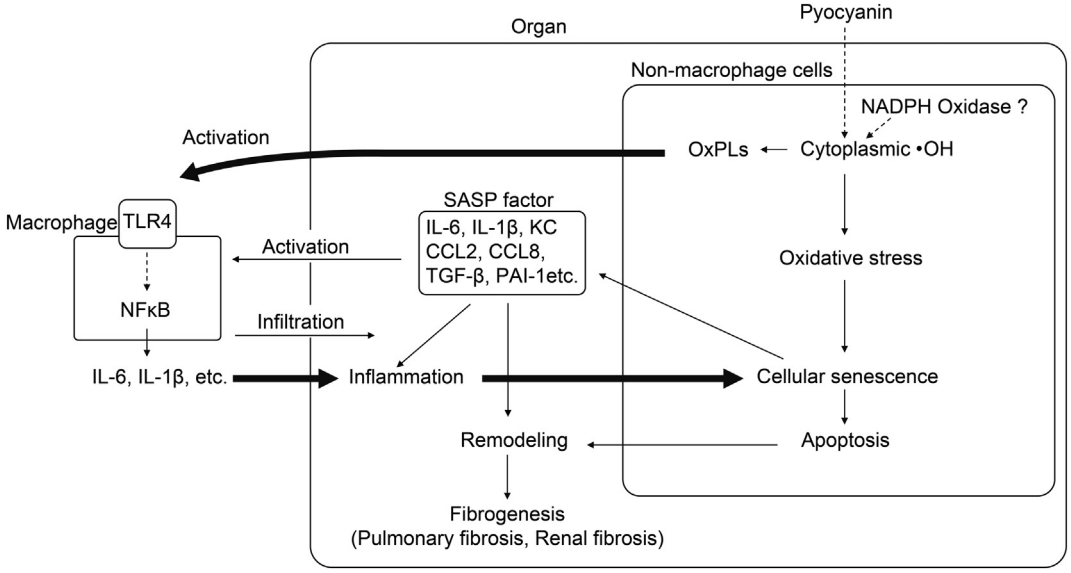

Fig. 6. Schematic pathway of fibrosis induction by cyto ·OH. Cyto ·OH promotes cellular senescence and generates OxPLs in the lungs and kidneys. Senescent cells release SASP factors, causing macrophage infiltration, however, the main pathway for macrophage infiltration is the activation of macrophages via OxPL/TLR4. Inflammatory cytokines are released by macrophages activated through OxPLs/TLR4, resulting in the aggravation of cellular senescence and inflammation and induction of apoptosis and fibrosis in the damaged tissues.

implicated in fibrogenesis through deposition of the ECM. However, both inflammation and fibrosis were inhibited by TA293, highlighting its role as a candidate anti-fibrotic agent with therapeutic potential.

One limitation of this study was that we did not identify OxPLs produced by cyto ·OH through lipid peroxidation, although we do provide indirect evidence for OxPL generation. Nevertheless, our data suggest that OxPLs act as lipid mediators exacerbating cellular senescence and inflammation induced by oxidative stress.

5. Conclusion

Our study suggests a mechanism whereby cyto ·OH-generated OxPLs act as lipid mediators to activate macrophages, serving to significantly exacerbate cyto ·OH-induced cellular senescence, inflammation, and apoptosis, and promote the progression of fibrogenesis. Our findings also indicate that TA293 is a promising molecule with potential therapeutic benefits due to its ·OH scavenging activity and should be further investigated in models of chronic inflammatory conditions and fibrosis.

Supplementary data to this article can be found online at https://doi.org/10.1016/j.lfs.2019.02.038.

Acknowledgements

Funding: This work was supported by the Japan Society for the Promotion of Science KAKENHI Grant in-Aid for Young Scientists (B) [grant number 24700434]; and the Science Research Promotion Fund from the Promotion and Mutual Aid Corporation for Private Schools of Japan.

Cactus Communications provided editorial support in the form of medical writing based on our detailed directions, collating our comments, copyediting, fact checking, and referencing.

Conflict of interest statement

The authors declare that there are no conflicts of interest.

References

[1] J.M. McCord, The evolution of free radicals and oxidative stress, Am. J. Med. 108 (2000) 652–659.
[2] M. Valko, C.J. Rhodes, J. Moncol, M. Izakovic, M. Mazur, Free radicals, metals and antioxidants in oxidative stress-induced cancer, Chem. Biol. Interact. 160 (2006) 1–40.
[3] E. Gammella, S. Recalcati, G. Cairo, Dual role of ROS as signal and stress agents: Iron tips the balance in favor of toxic effects, Oxidative Med. Cell. Longev. 2016 (2016).
[4] W.W. Dong, Y.Q. Zhang, X.Y. Zhu, Y.F. Mao, X.J. Sun, Y.J. Liu, L. Jiang, Protective effects of hydrogen-rich saline against lipopolysaccharide-induced alveolar epithelial-to-mesenchymal transition and pulmonary fibrosis, Med. Sci. Monit. 19 (2017) 2357–2364.
[5] Y. Ohta, K. Yashiro, T. Kobayashi, K. Inui, J. Yoshino, Protective effect of N,N'-dimethylthiourea against stress-induced gastric mucosal lesions in rats, Fundam. Clin. Pharmacol. 31 (2017) 319–328.
[6] L.H. Wu, P. Li, Q.L. Zhao, J.L. Piao, Y.F. Jiao, M. Kadowaki, T. Kondo, Arbutin, an intracellular hydroxyl radical scavenger, protects radiation-induced apoptosis in human lymphoma U937 cells, Apoptosis 19 (2014) 1654–1663.
[7] S. Turnbull, B.J. Tabner, O.M. El-Agnaf, S. Moore, Y. Davies, D. Allsop, Alpha-Synuclein implicated in Parkinson's disease catalyses the formation of hydrogen peroxide in vitro, Free Radic. Biol. Med. 30 (2001) 1163–1170.
[8] M. Marlatt, H.G. Lee, G. Perry, M.A. Smith, X. Zhu, Sources and mechanisms of cytoplasmic oxidative damage in Alzheimer's disease, Acta Neurobiol. Exp. (Wars) 64 (2004) 81–87.
[9] T. Sakai, J. Imai, T. Ito, H. Takagaki, M. Ui, S. Hatta, The novel antioxidant TA293 reveals the role of cytoplasmic hydroxyl radicals in oxidative stress-induced senescence and inflammation, Biochem. Biophys. Res. Commun. 482 (2017) 1183–1189.
[10] D. Oikawa, R. Akai, M. Tokuda, T. Iwawaki, A transgenic mouse model for monitoring oxidative stress, Sci. Rep. 2 (2012) 229.
[11] T. Iwawaki, R. Akai, D. Oikawa, T. Toyoshima, M. Yoshino, M. Suzuki, N. Takeda, T.O. Ishikawa, Y. Kataoka, K. Yamamura, Transgenic mouse model for imaging of interleukin-1β-related inflammation in vivo, Sci. Rep. 5 (2015) 17205.
[12] Y. Imai, K. Kuba, G.G. Neely, R. Yaghubian-Malhami, T. Perkmann, G. van Loo, M. Ermolaeva, R. Veldhuizen, Y.H. Leung, H. Wang, H. Liu, Y. Sun, M. Pasparakis, M. Kopf, C. Mech, S. Bavari, J.S. Peiris, A.S. Slutsky, S. Akira, M. Hultqvist, R. Holmdahl, J. Nicholls, C. Jiang, C.J. Binder, J.M. Penninger, Identification of oxidative stress and toll-like receptor 4 signaling as a key pathway of acute lung injury, Cell 133 (2008) 235–249.
[13] S. Nakamura, N. Kondo, Y. Yamaguchi, M. Hashiguchi, K. Tanabe, C. Ushiroda, M. Kawahashi-Tokuhisa, K. Yui, M. Miyakoda, T. Oku, Daily feeding of fructooligosaccharide or glucomannan delays onset of senescence in SAMP8 mice, Gastroenterol. Res. Pract. 2014 (2014) (2014).
[14] A. Biernacka, M. Dobaczewski, N.G. Frangogiannis, TGF-β signaling in fibrosis, Growth Factors 29 (2011) 196–202.
[15] K. Richter, T. Kietzmann, Reactive oxygen species and fibrosis: further evidence of a significant liaison, Cell Tissue Res. 365 (2016) 591–605.
[16] V. Sánchez-Valle, N.C. Chávez-Tapia, M. Uribe, N. Méndez-Sánchez, Role of oxidative stress and molecular changes in liver fibrosis: a review, Curr. Med. Chem. 19 (2012) 4850–4860.
[17] L. Villegas, T. Stidham, E. Nozik-Grayck, Oxidative stress and therapeutic development in lung diseases, J. Pulm. Respir. Med. 4 (2014) 194.
[18] K. Fukuhara, T. Nakashima, M. Abe, T. Masuda, H. Hamada, H. Iwamoto, K. Fujitaka, N. Kohno, N. Hattori, Suplatast tosilate protects the lung against hyperoxic lung injury by scavenging hydroxyl radicals, Free Radic. Biol. Med. 106 (2017) 1–9.
[19] M. Muller, Premature cellular senescence induced by pyocyanin, a redox-active Pseudomonas aeruginosa toxin, Free Radic. Biol. Med. 41 (2006) 1670–1677.
[20] S. Enami, Y. Sakamoto, A.J. Colussi, Fenton chemistry at aqueous interfaces, Proc. Natl. Acad. Sci. U. S. A. 111 (2014) 623–628.
[21] S. Pushpakumar, L. Ren, S. Kundu, A. Gamon, S.C. Tyagi, U. Sen, Toll-like receptor 4 deficiency reduces oxidative stress and macrophage mediated inflammation in hypertensive kidney, Sci. Rep. 7 (2017) 6349.
[22] M. Manček-Keber, M. Frank-Bertoncelj, I. Hafner-Bratkovic, A. Smole, N. Pirher, S. Hayer, V. Kralj-Igliv, B. Rozman, N. Ilc, S. Horvat, R. Jerala, Toll-like receptor 4 senses oxidative stress mediated by the oxidation of phospholipids in extracellular vesicles, Sci. Signal. 8 (2015) ra60.
[23] Y. Octavia, H.P. Brunner-La Rocca, A.L. Moens, NADPH oxidase-dependent oxidative stress in the failing heart: from pathogenic roles to therapeutic approach, Free Radic. Biol. Med. 52 (2012) 291–297.
[24] A. Panday, M.K. Sahoo, D. Osorio, S. Batra, NADPH oxidases: an overview from structure to innate immunity-associated pathologies, Cell. Mol. Immunol. 12 (2015) 5–23.
[25] L. Hecker, R. Vittal, T. Jones, R. Jagirdar, T.R. Luckhardt, J.C. Horowitz, S. Pennathur, F.J. Martinez, V.J. Thannickal, NADPH oxidase-4 mediates myofibroblast activation and fibrogenic responses to lung injury, Nat. Med. (9) (2009) 1077–1081.
[26] M. Sedeek, G. Callera, A. Montezano, A. Gutsol, F. Heitz, C. Szyndralewiez, P. Page, C.R. Kennedy, K.D. Burns, R.M. Touyz, R.L. Hébert, Critical role of Nox4-based NADPH oxidase in glucose-induced oxidative stress in the kidney: implications in type 2 diabetic nephropathy, Am. J. Physiol. Ren. Physiol. 299 (2010) F1348–F1358.